Received: 29 January 2019 | Revised: 18 October 2019 | Accepted: 18 November 2019

DOI: 10.1002/jrs.5804

RESEARCH ARTICLE

WILEY Journal of RAMAN SPECTROSCOPY

Single-layer multiple-kernel-based convolutional neural network for biological Raman spectral analysis

Won Bum Sohn[1] | **Soo Yeol Lee**[1] | **Soogeun Kim**[2]

[1] Department of Biomedical Engineering, Kyung Hee University, Yongin, South Korea

[2] Department of Biomedical Engineering, Kyung Hee University, Seoul, South Korea

Correspondence
Soo Yeol Lee, Department of Biomedical Engineering, Kyung Hee University, Yongin 17104, South Korea.
Email: sylee01@khu.ac.kr

Soogeun Kim, Department of Biomedical Engineering, Kyung Hee University, Seoul 02447, South Korea.
Email: sigamda@khu.ac.kr

Funding information
National Research Foundation of Korea, Grant/Award Number: 2018R1C1B6008568, 2019R1F1A1048615

Abstract

In this study, we propose a single-layer multiple-kernel-based convolutional neural network (SLMK-CNN) as an analysis tool for biological Raman spectra. We investigated the characteristics of SLMK-CNN and then analyzed and classified the biological Raman spectra by optimizing the structure of SLMK-CNN. We have found that the kernel size used in SLMMK-CNN plays an important role in changing the characteristics of Raman spectra such as intensity and peak position. As a result, the kernel size affects the classification performance and histological interpretation of biological Raman spectra. We also evaluated the classification performance of SLMK-CNN using Raman spectra obtained from the porcine skin samples irradiated by an ultraviolet (UV) source for different time. For three sample groups according to UV irradiation time (0, 10, and 24 hr), SLMK-CNN showed the classification accuracy of 96.4% and 92.5% for the preprocessed and raw Raman spectra, respectively. This is superior to other classification methods such as single-layer single-kernel-based CNN and principal component-linear discriminant analysis in this study.

KEYWORDS

bio-sample, classification, convolutional neural networks, multiple kernel, Raman spectra

1 | INTRODUCTION

Since the discovery of Raman scattering[1] in 1928, Raman spectroscopy has been applied to analyze and classify target materials in a variety of fields, including chemistry, food, environment, and medicine.[2–6] Naturally, a number of classification methods for Raman spectra have also been studied.[7–10] The most widely used classification methods are linear discriminant analysis (LDA), artificial neural networks (ANNs), and support vector machines (SVM). Ghita et al.[7] developed the multivariate statistical method based on principal component analysis (PCA) and LDA for noninvasive monitoring of living neural stem cells in vitro through classification of undifferentiated neural stem cells and glial cells. Gniadecka et al.[8] used ANN, a pattern recognition tool, to classify skin lesions such as melanoma, pigmented nevi, basal cell carcinoma, and seborrheic keratosis. Widjaja et al.[9] reported that using SVM in Raman spectroscopy could improve the ability to classify multiple histopathological tissues of the colon. In general, most classification methods require the preprocessing procedure of raw Raman spectra. This is because the classification accuracy is greatly improved by preprocessing procedures such as smoothing, baseline correction, and normalization. In particular, in the case of bio-samples, preprocessing procedures are almost necessary because unwanted fluorescent background signals overwhelm Raman signals. However, it is difficult to find proper conditions of preprocessing procedures.

Liu et al.[11] presented the classification method based on deep convolutional neural network (CNN) that automatically classifies chemicals without the preprocessing

procedure of Raman spectra. Using raw Raman spectra of the chemicals, they showed that the classification accuracy of the deep CNN (93%) was much better than that of other methods such as SVM (52%) and random forest (39%). However, Liu's CNN was difficult to interpret chemically and/or molecularly because the raw Raman spectra were significantly distorted by the deep CNN structure. For theoretical interpretation of Raman spectra, it is important to correlate changes in chemical composition with changes in Raman spectra. On the contrary, Acquarelli et al.[12] proposed a shallow CNN structure that uses a single convolutional layer only. This study has shown that the theoretical interpretation is possible using the shallow CNN through classification analysis of various food samples. However, the preprocessing procedure is required for high classification accuracy.

In this study, we propose a single-layer multiple-kernel-based CNN (SLMK-CNN) that can simultaneously classify and interpret biological Raman spectra. We use a single convolutional layer like Acquarelli's study but uses five different-sized kernels at the same time on the single convolutional layer. Each input Raman spectrum has a one-dimensional (1-D) array so that the 1-D kernel of five sizes is used in SLMK-CNN: 1×3, 1×7, 1×13, 1×27, and 1×45. We have investigated the characteristics of each kernel size and have evaluated the classification performance of SLMK-CNN using three groups of Raman spectra with different ultraviolet (UV) irradiation times for porcine skin samples. Both preprocessed and raw Raman spectra were considered for evaluation of classification performance.

2 | MATERIALS AND METHODS

2.1 | Measurement of Raman spectra from UV-irradiated bio-samples

When UV-induced harmful responses of biological skin are investigated,[13] classification of the exposure level of the skin to UV may provide some information for early-stage skin damage caused by UV irradiation. We took 12 porcine skin samples from a middle-sized pig at a slaughterhouse and used them as bio-samples in this study. The size of each bio-sample was about 20 mm × 20 mm × 1 mm. In order to assign a differentiable group, we set three different UV irradiation conditions to the bio-samples: (a) without UV irradiation (00H), (b) with UV irradiation for 10 hr (10H), and (c) with UV irradiation for 24 hr (24H). We used a 20-W UV source with the length of 550 cm for the irradiation. At each UV irradiation condition, we measured Raman spectra at 10 random spots of each bio-sample. As a result, we obtained 120 Raman spectra at each UV irradiation condition. In Figure S1, the Raman measurement procedure for three different UV irradiation conditions is shown in detail. For the control group, Raman spectra were additionally measured at 10 and 24 hr for non-UV-irradiated bio-samples. The bio-samples were put in distilled water except when measuring Raman spectra.

Raman spectra from the bio-samples were measured by a confocal Raman microscope system. For a Raman excitation source, we used a 785-nm laser (I0785MM0350MF, Innovative Photonic Solutions, USA) with laser power of 50 mW and spot diameter of 120 μm on the bio-sample surface. We collected the Raman signal from the bio-sample using a 10× objective lens with numerical aperture of 0.3 (LDJ 10, Shibuya Optical Co. Ltd, Japan) and detected the signal using a Czerny-Turner spectrograph (SR-303i-A, Andor Technology, UK) with a low dark-current deep-depletion CCD (iVac, Andor Technology, UK). We acquired each Raman spectrum in the range from 600 to 1,800 cm^{-1} with the wavenumber resolution of 1.8 cm^{-1} and the acquisition time of 60 s.

To preprocess the raw Raman spectra, we subtracted the instrument and CCD noise signal from the raw Raman signal and then applied the Savitzky–Golay smoothing[14] and the improved multipolynomial baseline correction[15] sequentially. We also applied vector normalization[10] to remove spectral variation caused by excitation source fluctuation. In vector normalization, the Euclidean norm of a Raman spectrum defined by the square root of the sum of the squared Raman intensities is calculated, and then each Raman intensity corresponding to a wavenumber is divided by the Euclidean norm in the entire wavenumber range.

2.2 | Single-layer multiple-kernel-based CNN

SLMK-CNN has a simple CNN structure consisting of a single convolutional layer, a single flatten layer, and two fully connected layers (see Figure 1). SLMK-CNN works with the following procedure. First of all, in the convolutional layer, the convolution between each element of the input Raman data and each element of the kernel is performed by shifting the kernel using a stride of 1 from the beginning to the last input element. Five different-sized kernels are used simultaneously in a single convolutional layer: 1×3, 1×7, 1×13, 1×27, and 1×45. In other words, one input is provided in parallel to kernels of different sizes as shown in Figure 1. The number of kernels is 8, 16, 32, 64, and 128 for the kernel of 1×3, 1×7, 1×13, 1×27, and 1×45, respectively, which is repeatedly applied to the input Raman data. Because the input Raman

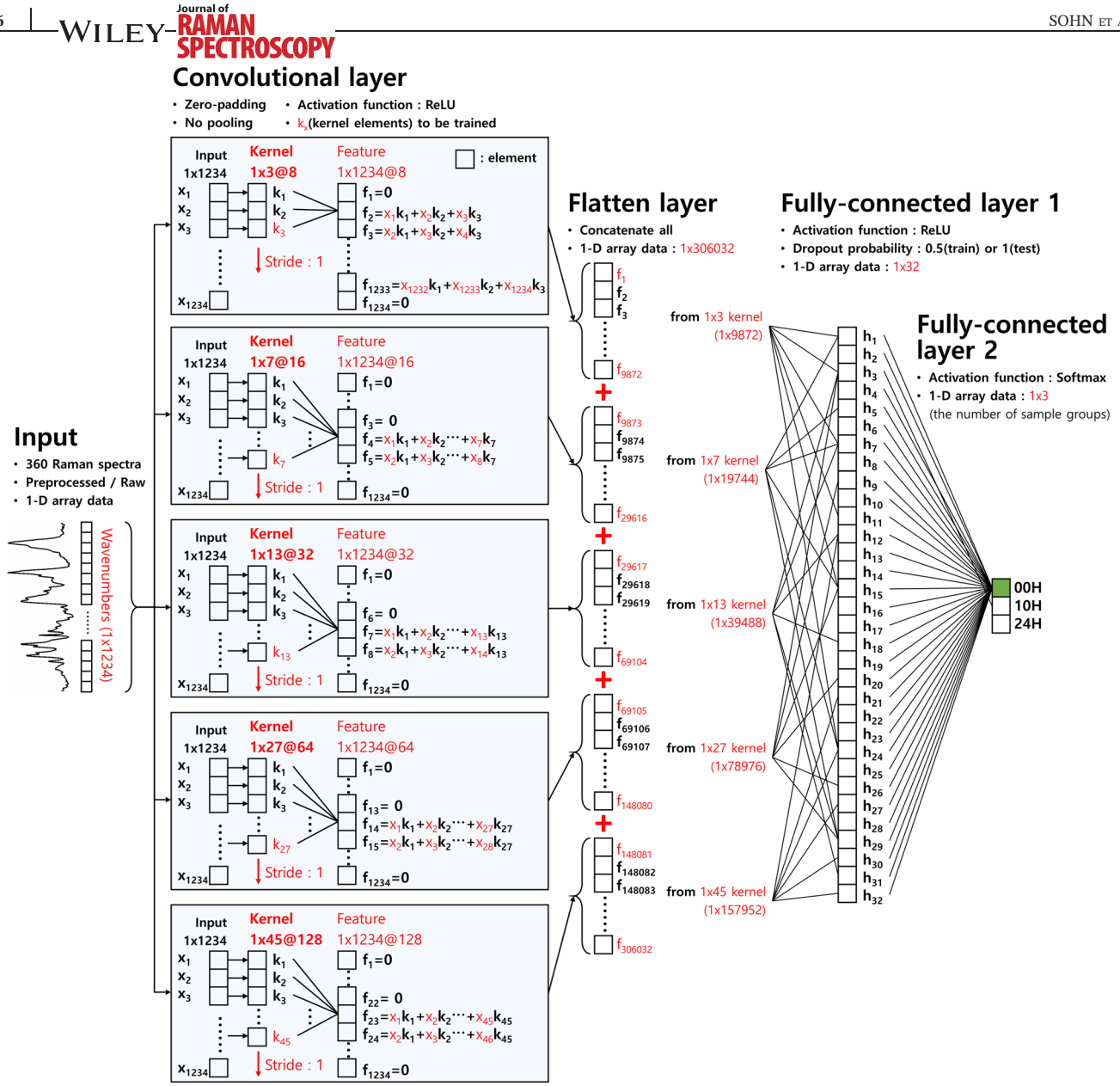

FIGURE 1 The detailed structure of single-layer multiple-kernel-based convolutional neural network (SLMK-CNN) consisting of a single convolutional layer with five different-sized kernels for feature extraction, a single flatten layer, and two fully connected layers for classification [Colour figure can be viewed at wileyonlinelibrary.com]

spectrum (1 × 1,234) is represented by a 1-D array, the kernel has a 1-D array format. The outcome of the convolution is called a feature. Through this convolutional procedure, 248 features are made for one input: 8 features from 1 × 3 kernel, 16 features from 1 × 7 kernel, 32 features from 1 × 13 kernel, 64 features from 1 × 27 kernel, and 128 features from 1 × 45 kernel. Due to the use of zero padding, each feature has 1 × 1,234 array size like the input Raman spectrum. All features are activated by the rectified linear unit (ReLU) that is commonly used as activation function for convolutional layers, and each activated feature has also 1 × 1,234 array size. In the flatten layer, all activated features (all outcomes of the ReLU) are concatenated and flattened into a 1-D array having 1 × 306,032 size. Then the first fully connected layer activates the flattened 1-D array data using the ReLU and reduces the flattened data size to 1 × 32 size. Finally, the second fully connected layer (output layer) uses a softmax activation function that is commonly used in an output layer for reliable classification because it provides normalized nonnegative probability values.[12] The number of elements in the output layer is 3 (i.e., 1 × 3 array data), which is equal to the number of sample groups. The detailed structure and procedure are shown in Figure 1.

A total of 360 Raman spectra were used for training and test of SLMK-CNN (120 from the 00H condition, 120 from the 10H condition, and 120 from the 24H condition). First, weights (i.e., values) for kernels in convolutional layer and

for two fully connected layers are randomly initialized from a normal distribution with a zero mean and standard deviation of 1×10^{-2}. Weights are then learned during the training of SLMK-CNN in a supervised manner using cross-entropy loss function and Adam algorithm, a stochastic gradient-based optimization technique.[16] The value of mini-batch size, learning rate and epoch for this training is 12, 1×10^{-4} and 150, respectively. The epoch value of 150 is selected through the criterion to prevent overfitting in SLMK-CNN using Figure S2a. The classification accuracy of the training is saturated, but that of the test has a maximum value at 150 epochs and then decreases. The 12-fold cross validation is used to obtain the classification accuracy. A regularization method called "dropout" is used in first fully connected layer to prevent overfitting (dropout probability = 0.5).[17] We have implemented the proposed CNN using TensorFlow.[18]

3 | RESULTS AND DISCUSSION

To understand the behavior of SLMK-CNN for classification, we first investigated the convolutional properties of each kernel size: 1×3, 1×7, 1×13, 1×27, and 1×45. Figure 2 shows the variation of the feature according to the kernel size at each sample group for raw (top 3)/preprocessed (bottom 3) input Raman data. From the results, we can find that the feature is strongly influenced by the kernel size. We observed four main convolutional properties with varying kernel sizes. As the kernel size increases, (a) the feature profile is smoothed, (b) the feature intensity increases over the range of all wavenumbers, (c) the peak position is shifted, and (d) the feature profile is distorted. These convolutional properties appear very similar across all conditions (i.e., conditions of three sample groups and raw/preprocessed input Raman data). By the analysis results of the features in Figure 2, it appears that SLMK-CNN learns the rate of change of Raman spectral information (Raman peak intensity, Raman peak position, and Raman spectral profile) with varying UV irradiation conditions (00H, 10H, and 24H).

We then investigated the effects of the convolutional properties on the classification of biological Raman spectra. Figure 3a shows the preprocessed input Raman data for three sample groups, shown as mean and standard deviation. We can easily observe that the means overlap over the range of all wavenumbers, as well as the standard deviations. This means that there is little chance to distinguish Raman data of one sample group from the other groups. The features by 1×3 kernel show very similar profile when compared with the preprocessed input Raman data except the peak intensity (see Figure 3b). On the other hand, for 1×45 kernel, the means between three sample groups are further separated, and even the standard deviation is separated in some wavenumber range (see the arrow in Figure 3c). The analysis results of relative standard deviation (RSD) in Figure 3d show that this result, in which the mean and standard deviation between the three sample groups are separated, is related to the change of kernel size. RSD is obtained by dividing the standard deviation by the mean. As the kernel size increases, the RSD decreases, which is believed to

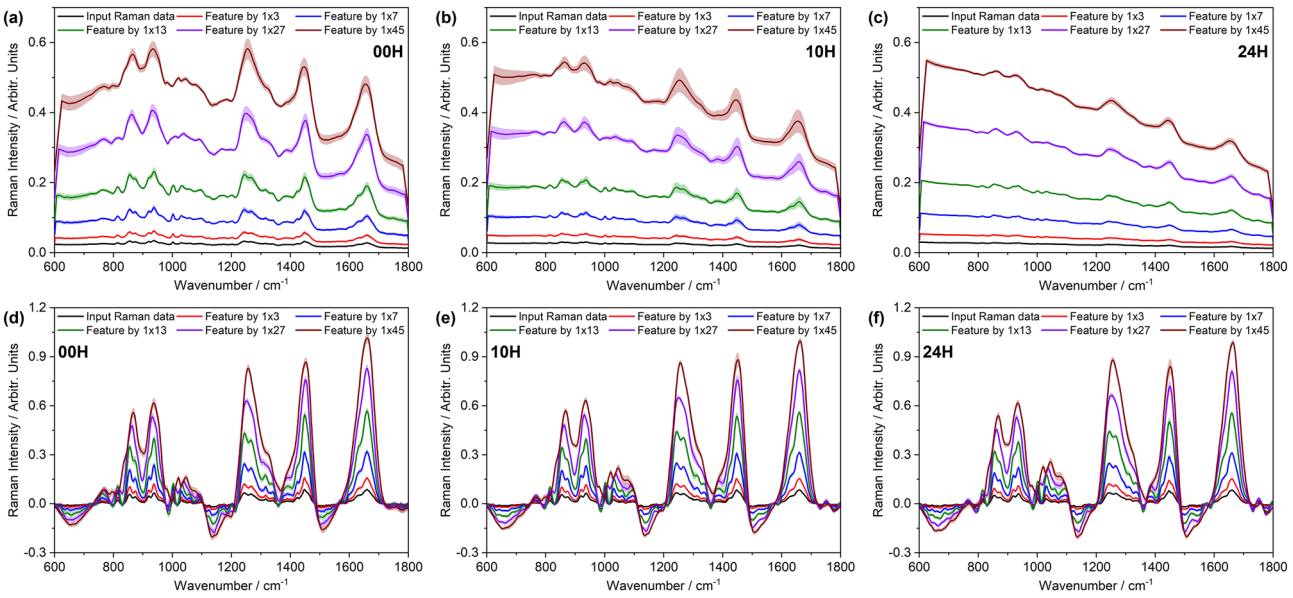

FIGURE 2 Variation of the feature according to the kernel size at each sample group (00H, 10H, and 24H) (a–c) for raw input Raman data and (d–f) for preprocessed input Raman data. Each solid line and filled area is the mean and standard deviation calculated for all features obtained at each kernel size [Colour figure can be viewed at wileyonlinelibrary.com]

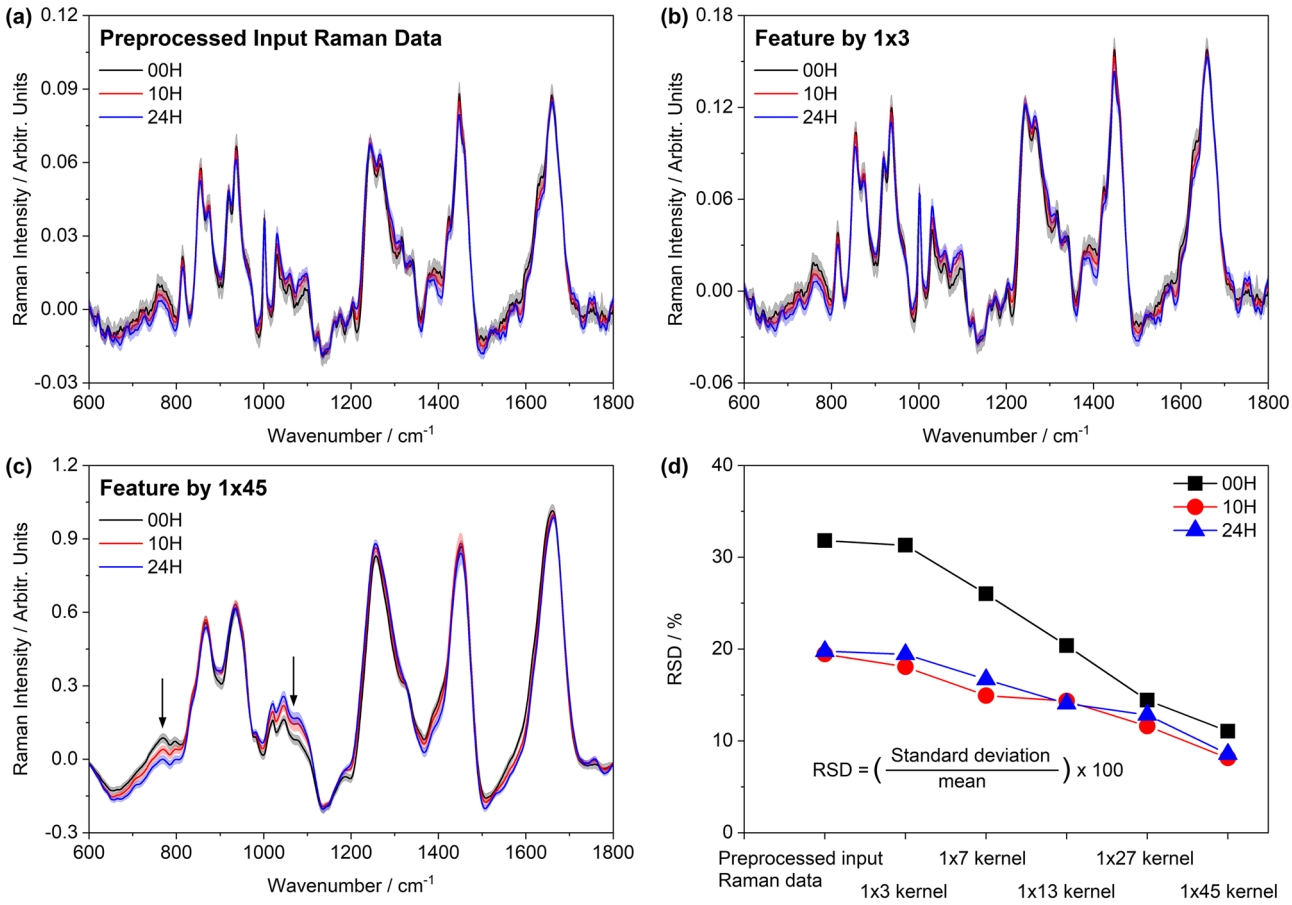

FIGURE 3 (a) Preprocessed input Raman data, (b) features by 1 × 3 kernel, and (c) features by 1 × 45 kernel according to three sample groups (00H, 10H, and 24H). (d) Variation of relative standard deviation (RSD) for features according to the kernel size [Colour figure can be viewed at wileyonlinelibrary.com]

be due to the strong smoothing effect of the larger kernel. In addition, the minimum value of *p* value by ANOVA test also decreases as the kernel size increases, as shown in Figure S3. From these results, we expect that the classification capability of SLMK-CNN will be improved by increasing the kernel size.

Figure 4a–c shows magnified views of Figure 3a–c in the range from 1,400 to 1,500 cm^{-1}. In Figure 4, the standard deviation is not indicated for the sake of clear visualization of the spectra. The Raman peak intensity at 1,447 cm^{-1} is decreasing with increasing the UV irradiation time, as can be noticed from Figure 4a. The photobleaching by the UV irradiation can occur so that raw signal including both the fluorescence and the Raman signal decrease with photobleaching time. However, Wang et al.[19] found that the fluorescence decreases monotonically with time while the Raman signal stays almost constant. In biological skin, the wavenumber at the range from 1,440 to 1,450 cm^{-1} is attributed to CH_2 deformation and/or cholesterol variation.[20] Shah and Rawal Mahajan[21] pointed out that exposure of skin to UV can lead to decrease of fatty acid and cholesterol synthesis in the skin. Figure 4d shows Raman spectra measured at 0, 10, and 24 hr without UV irradiation, and there is little change in peak intensity at 1,447 cm^{-1} unlike Figure 4a. Therefore, the decrease observed in Figure 4a is likely to be due to a decrease in cholesterol by UV irradiation, rather than simply degradation of the sample over time without UV irradiation. The *p* value profiles for three sample groups with and without UV irradiation also show that the change is greater at Raman peak of 1,447 cm^{-1} when UV is irradiated (see Figure S4).

Figure 4b for 1 × 3 kernel shows that there is little change in relative peak intensity at 1,447 cm^{-1} between groups as compared with Figure 4a. On the other hand, for 1 × 45 kernel shown in Figure 4c, the difference in the peak intensity between the groups is relatively decreased, which may adversely affect the classification between the groups. In terms of the classification, the result of Figure 4c is inconsistent with the result in Figure 3c. Thus, using multiple kernels of different sizes may result in better classification performance than using a single kernel through complementary effects between kernels of different sizes. The confusion matrix in Table 1, produced by 12-fold cross validation, shows the classification performance of single-kernel and SLMK-

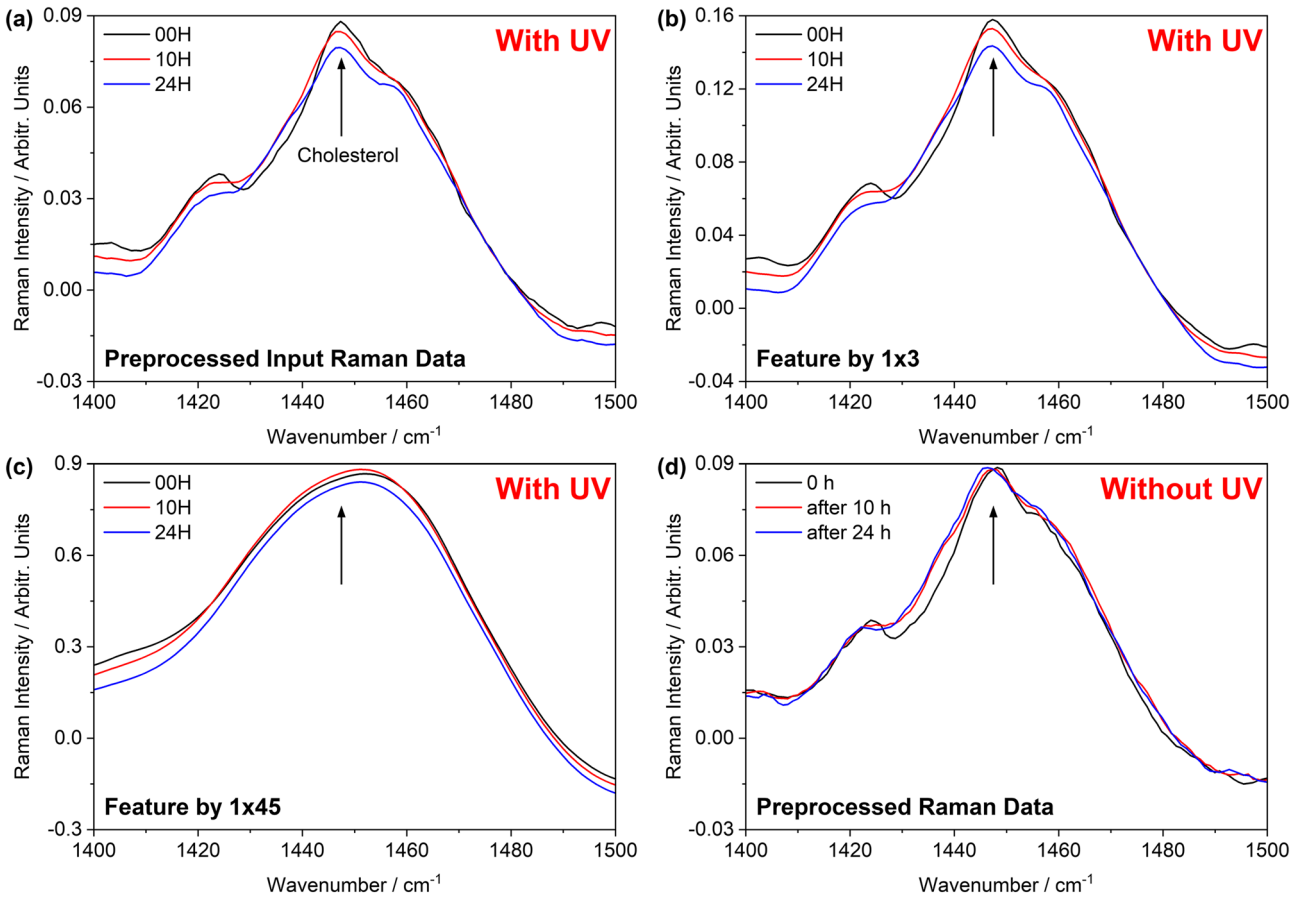

FIGURE 4 Magnified views of (a) preprocessed input Raman data, (b) features by 1 × 3 kernel, and (c) features by 1 × 45 kernel according to three sample groups (00H, 10H, and 24H) in the wavenumber range from 1,400 to 1,500 cm^{-1}. (d) Preprocessed Raman data obtained at 0, 10, and 24 hr without ultraviolet irradiation [Colour figure can be viewed at wileyonlinelibrary.com]

CNN. The amount of training data for 12-fold cross validation is 348. The total number of weights of SLMK-CNN is 250 (see Table S1). The ratio between weights to be trained and the amount of training data is 1.39 (=348/250). This weight number is used in SLMK-CNN to obtain high classification accuracy without overfitting (see Figure S2b). In both preprocessed and raw input Raman data, the classification accuracy is improved when SLMK-CNN is used. Particularly, the improvement is much higher in the case of raw input Raman data. SLMK-CNN provides more than 90% classification accuracy even with raw input Raman data. The classification results of SLMK-CNN were compared with those of conventional method like principal component-linear discriminant analysis (PC-LDA) because the results of SLMK-CNN can be biased due to the small sample size. The confusion matrix of PC-LDA is represented in Table S2. For preprocessed input Raman data, the classification accuracy of SLMK-CNN and PC-LDA is almost the same. However, for raw input Raman data, the classification accuracy is different. Further studies are needed to increase the generalization of SLMK-CNN.

TABLE 1 Confusion matrix of single-kernel CNN and SLMK-CNN

	Preprocessed input Raman data						Raw input Raman data					
	Single-kernel CNN (1 × 45 kernel)			SLMK-CNN			Single-kernel CNN (1 × 45 kernel)			SLMK-CNN		
	00H	10H	24H	00H	10H	24H	00H	10H	24H	00H	10H	24H
00H	119	0	6	119	0	0	113	22	10	118	11	0
10H	1	108	12	1	113	5	7	78	1	2	97	2
24H	0	12	102	0	7	115	0	20	109	0	12	118
Accuracy	91.4%			96.4%			83.3%			92.5%		

Abbreviation: SLMK-CNN, single-layer multiple-kernel-based convolutional neural network.

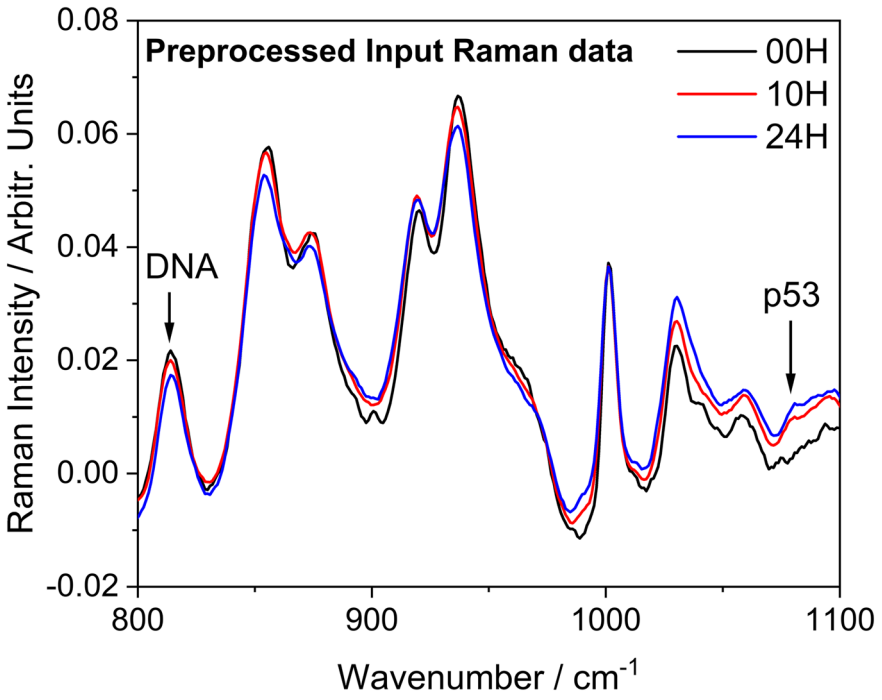

FIGURE 5 Spectral variations of Raman spectra according to ultraviolet irradiation conditions (00H, 10H, and 24H) in the wavenumber range from 800 to 1,100cm^{-1}. [Colour figure can be viewed at wileyonlinelibrary.com]

Representation learning will allow SLMK-CNN to achieve better generalization by learning representations of the input Raman data that make it easier to extract useful Raman spectral information. The generalization performance of representation learning has been demonstrated in many previous studies in which the following learning algorithms were used: unsupervised learning algorithms such as deep belief net or stacked denoising autoencoder and transfer learning algorithm.[22–24] In addition, generalization performance is usually improved by providing a larger quantity of representative data.[23] This study used roughly two orders of magnitude less than the previous studies, but SLMK-CNN has succeeded in extracting useful Raman spectral information from input Raman data (see Figure 2). Therefore, as the number of training data increases, the generalization performance of SLMK-CNN is expected to improve.

Histological interpretation is as much important as classification in biological Raman analysis. This is because the changes in Raman peak intensity, Raman peak position, and/or Raman spectral profile are strongly related to the changes in chemical composition of biological substrates such as proteins, lipids, and nucleic acids. The analysis of Raman spectra can give histological information for bio-samples. If skin is constantly irradiated to UV light to the extent that the UV dose finally exceeds the threshold damage response of the skin, DNA and cellular damage in keratinocytes occurs in addition to aforementioned reduction of cholesterol.[21,25] Upon UV irradiation higher than the threshold, p53 proteins are activated for cell cycle arrest, DNA damage repair, and apoptosis.[21,25] These UV-induced biological variation, such as DNA damage, p53 activation, and cholesterol decrease, can be detected by Raman spectroscopy. It is known that DNA,[26,27] p53 protein,[28,29] and cholesterol[20] are assigned to 814, 1,080, and 1,447 cm^{-1} of wavenumber, respectively. Those wavenumbers are all included in the Raman spectra measured in this study.

Figures 4a and 5 show the variation of Raman spectra according to UV irradiation conditions (00H, 10H, and 24H). As UV irradiation time increases, the Raman peak intensity at 814 and 1,447 cm^{-1} is decreased, which can be attributed to the DNA damage and the decrease of cholesterol synthesis caused by UV irradiation. On the other hand, the Raman peak intensity at 1,080 cm^{-1} is increased, possibly due to the activation of p53 protein caused by DNA damage. This UV-induced spectral variation is preserved in the feature of small-sized kernels (1×3, 1×7, and 1×13) but is distorted in the feature of large-sized kernels (1×27 and 1×45), as shown in Figure S5. In Figure 4 c, not only the peak position of 1,447 cm^{-1} (cholesterol) is shifted, but also the order of peak intensity is changed between 00H and 10H. The peaks at 814 cm^{-1} (DNA) and 1,080 cm^{-1} (p53) widen or even disappear as the kernel size increases (see Figure S5). These results indicate that the CNN consisting of a single large-sized kernel can significantly distort the spectral information that enables histological interpretation.

4 | CONCLUSION

In this study, we proposed SLMK-CNN using five different-sized kernels at the same time on a single convolutional

layer to classify and interpret biological Raman spectra. Through the investigation of convolutional properties of each kernel size (1 × 3, 1 × 7, 1 × 13, 1 × 27, and 1 × 45), we found that the classification performance was improved by the complementary effects of the multiple kernels of different sizes. In terms of histological interpretation, because only using a single large-sized kernel can distort the spectral information (Raman peak intensity, Raman peak position, and/or Raman spectral profile), we suggest that the multiple kernels of different sizes are used simultaneously in a single convolutional layer. Therefore, further studies are needed to improve the generalization, but SLMK-CNN using five different-sized kernels is expected to not only accurately classify biological Raman spectra but also to allow histological interpretation.

DISCLOSURES

All authors declare no conflicts of interest or financial relationships to disclose.

ACKNOWLEDGEMENTS

This work was supported by the National Research Foundation of Korea (NRF) grant funded by the Korean government (2019R1F1A1048615 and 2018R1C1 B6008568).

ORCID

Soogeun Kim https://orcid.org/0000-0001-5483-6661

REFERENCES

[1] C. V. Raman, *Indian J. Phys.* **1928**, *2*, 387.

[2] D. V. Petrov, *Spectrochim. Acta Part A Mol. Biomol. Spectrosc.* **2018**, *191*, 573.

[3] O. Anjos, A. J. A. Santos, V. Paixão, L. M. Estevinho, *Talanta* **2018**, *178*, 43.

[4] R. L. Frost, T. Kloprogge, M. L. Weier, W. N. Martens, Z. Ding, H. G. H. Edwards, *Spectrochim. Acta Part A Mol. Biomol. Spectrosc.* **2003**, *59*, 2241.

[5] J. Binoy, I. Hubert Joe, V. S. Jayakumar, O. F. Nielsen, J. Aubard, *Laser Phys. Lett.* **2005**, *2*, 544.

[6] S. Cînta-Pînzaru, N. Peica, B. Küstner, S. Schlücker, M. Schmitt, T. Frosch, J. H. Faber, G. Bringmann, J. Popp, *J. Raman Spectrosc.* **2006**, *37*, 326.

[7] A. Ghita, F. C. Pascut, M. Mather, V. Sottile, I. Notingher, *Anal. Chem.* **2012**, *84*, 3155.

[8] M. Gniadecka, P. A. Philipsen, S. Wessel, R. Gniadecki, H. C. Wulf, S. Sigurdsson, O. F. Nielsen, D. H. Christensen, J. Hercogova, K. Rossen, H. K. Thomsen, L. K. Hansen, *J. Invest. Dermatol.* **2004**, *122*, 443.

[9] E. Widjaja, W. Zheng, Z. Huang, *Int. J. Oncol.* **2008**, *32*, 653.

[10] R. Gautam, S. Vanga, F. Ariese, S. Umapathy, *EPJ Tech. Instrum.* **2015**, *2*, 8.

[11] J. Liu, M. Osadchy, L. Ashton, M. Foster, C. J. Solomon, S. J. Gibson, *Analyst* **2017**, *142*, 4067.

[12] J. Acquarelli, T. van Laarhoven, J. Gerretzen, T. N. Tran, L. M. C. Buydens, E. Marchiori, *Anal. Chim. Acta* **2017**, *954*, 22.

[13] E. J. Kim, X.-J. Jin, Y. K. Kim, I. K. Oh, J. E. Kim, C.-H. Park, J. H. Chung, *J. Dermatol. Sci.* **2010**, *57*, 19.

[14] J. Addis, N. Mohammed, O. Rotimi, D. Magee, A. Jha, V. Subramanian, *Biomed. Opt. Express* **2016**, *7*, 2022.

[15] J. Zhao, H. Lui, D. I. McLean, H. Zeng, *Appl. Spectrosc.* **2007**, *61*, 1225.

[16] D. P. Kingama, J. L. Ba, Int. Conf. Learn. Represent. **2015**, arXiv preprint arXiv:1412.6980.

[17] N. Srivastava, G. Hinton, A. Krizhevsky, R. Salakhutdinov, *J. Mach. Learn. Res.* **2014**, *15*, 1929.

[18] TensorFlow, https://www.tensorflow.org/.

[19] H. Wang, J. Zhao, A. M. D. Lee, H. Lui, H. Zeng, *Photodiagnosis Photodyn. Ther.* **2012**, *9*, 299.

[20] S. Tfaili, C. Gobinet, G. Josse, J.-F. Angiboust, M. Manfait, O. Piot, *Analyst* **2012**, *137*, 3673.

[21] H. Shah, S. Rawal Mahajan, *Biomed. Aging Pathol.* **2013**, *3*, 161.

[22] D. Erhan, Y. Bengio, A. Courville, P.-A. Manzagol, P. Vincent, S. Bengio, *J. Mach. Learn. Res.* **2010**, *11*, 625.

[23] Y. Bengio, A. Courville, P. Vincent, *IEEE Trans. Pattern Anal. Mach. Intell.* **2013**, *35*, 1798.

[24] A. P. Raulf, J. Butke, C. Küpper, F. Großerueschkamp, K. Gerwert, A. Mosig, *bioRxiv* **2019**, *n/a*, 584227.

[25] J. D'Orazio, S. Jarrett, A. Amaro-Ortiz, T. Scott, *Int. J. Mol. Sci.* **2013**, *14*, 12222.

[26] Y.-D. Zhao, D.-W. Pang, S. Hu, Z.-L. Wang, J.-K. Cheng, Y.-P. Qi, H.-P. Dai, B.-W. Mao, Z.-Q. Tian, J. Luo, Z.-H. Lin, *Anal. Chim. Acta* **1999**, *388*, 93.

[27] I. Notingher, C. Green, C. Dyer, E. Perkins, N. Hopkins, C. Lindsay, L. L. Hench, *J. R. Soc. Interface* **2004**, *1*, 79.

[28] F. Domenici, A. R. Bizzarri, S. Cannistraro, *Anal. Biochem.* **2012**, *421*, 9.

[29] P. Owens, N. Phillipson, J. Perumal, G. M. O'Connor, M. Olivo, *Biosensors* **2015**, *5*, 664.

SUPPORTING INFORMATION

Additional supporting information may be found online in the Supporting Information section at the end of the article.

How to cite this article: Sohn WB, Lee SY, Kim S. Single-layer multiple-kernel-based convolutional neural network for biological Raman spectral analysis. *J Raman Spectrosc*. 2020;51:414–421. https://doi.org/10.1002/jrs.5804